

Interpretable Apprenticeship Learning from Heterogeneous Decision-Making via Personalized Embeddings

Rohan Paleja, Andrew Silva, Letian Chen, Matthew Gombolay

Georgia Institute of Technology

{rpaleja3, andrew.silva, letian.chen, mgombolay3}@gatech.edu

Abstract

Advances in learning from demonstration (LfD) have enabled intelligent agents to learn decision-making strategies through observation. However, humans exhibit heterogeneity in their decision-making criteria, leading to demonstrations with significant variability. We propose a personalized apprenticeship learning framework that automatically infers an interpretable representation of all human task demonstrators by extracting latent, human-specific decision-making criteria specified by an inferred, personalized embedding. We achieve near-perfect LfD accuracy in synthetic domains and 89.02% accuracy on a real-world planning domain, significantly outperforming state-of-the-art benchmarks. Further, a user study conducted to assess the interpretability of different types of decision-making models finds evidence that our methodology produces both interpretable ($p < 0.04$) and highly usable models ($p < 0.05$).

1 Introduction

The field of learning from demonstration (LfD) attempts to capture domain-expert knowledge directly from demonstration. However, prior apprenticeship learning frameworks have been unable to account for the fact that human experts – who have different skills and habits – can show significant variability in their demonstrations while also exhibiting some commonalities in their approaches. For example, prior work learning auto-pilot behavior from commercial aviators found pilots executing the same flight plan created such heterogeneity as to make it more practical to learn from a single trajectory and disregard the remaining data [Sammut et al., 2002].

Only recently have some researchers begun to directly address the challenges of decision-maker heterogeneity for LfD [Nikolaidis et al., 2015, Li et al., 2017, Tamar et al., 2018]. For example, Nikolaidis et al. [2015] first used an expectation maximization formulation to cluster decision-maker behavior before applying inverse reinforcement learning (IRL) for each cluster k . Negatively, this approach requires interaction with an environment model and the IRL algorithm only has access to $1/k^{th}$ of the data to learn from,

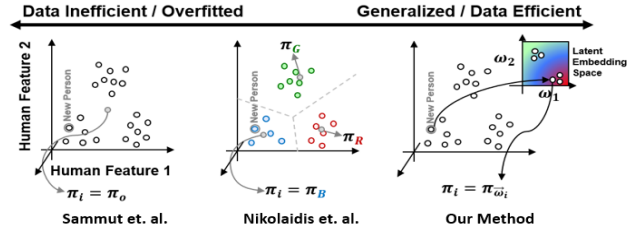


Figure 1: Approaches to LfD: (Left) Assume homogeneity [Sammut et al., 2002], (Center) Partition to semi-homogeneous clusters [Nikolaidis et al., 2015], (Right) Personalized embeddings (ours).

which significantly inhibits learning for high-dimensional problems. On the other hand, Li et al. [2017] attempts to learn a one-size-fits-all model that uses latent, discrete embeddings to tease out “modes” in decision-making. Nonetheless, we show in Section 5 that these works leave much to be desired in terms of imitation performance.

In this work, we develop a data-efficient LfD approach for heterogeneous decision-making; moreover, we formulate our method to be human-interpretable to provide a level of intelligibility and transparency [Bhatt et al., 2019] to the human expert demonstrators. Our learning architecture, which we call “personalized neural trees,” is designed to allow for conversion in post-training to a simple decision tree. This decision tree is then used both as the learned model for imitation and as its own interpretation [Letham et al., 2015], which reduces algorithm aversion in safety-critical domains.

In overcoming the limitations of prior work in addressing heterogeneity in LfD, our contributions are three-fold:

1. A personalized and interpretable apprenticeship learning framework for heterogeneous learning from demonstration (HLfD) that can outperform previous state-of-the-art LfD approaches in both synthetic and real-world domains (by a margin of $\sim 54\%$ and $\sim 13\%$, respectively) through the use of personalized embeddings without constraining the number of styles.
2. Methodology for converting a personalized neural tree into an interpretable representation that directly translates decision-making behavior. Our discretized trees also outperform previous benchmarks in both our synthetic and real-world domains.
3. A user study that shows our post-processed interpretable

trees are more interpretable ($p < 0.04$), easier to follow ($p < 0.05$), and quicker to validate ($p < 0.001$) than their black box neural network counterparts.

We evaluate our approach on three problems: A low-dimensional environment, a job scheduling environment with a mock experts’ scheduling heuristics, and a real-world dataset of behavior in a pickup-dropoff taxi domain.

2 Background

LfD mechanisms are often based on a Markov Decision Process (MDP), a five-tuple $M = \langle S, A, T, \gamma, R \rangle$ where S is a set of states, A is a set of actions, $T : S \times A \times S \rightarrow [0, 1]$ is a transition function, where $T(s, a, s')$ is the probability of being in state s' after executing action a in state s , $R : S \rightarrow \mathbb{R}$ (or $R : S \times A \rightarrow \mathbb{R}$) is the reward function, and $\gamma \in [0, 1]$ is the discount factor. The goal in LfD is to receive both a set of trajectories provided by a human demonstrator $\{\langle s_t, a_t \rangle, \text{ for time step } t \in \{1, 2, \dots\}\}$ as well as an MDP sans reward function R , and then to recover a policy that can predict the correct state-action sequence a human would take in a novel situation, thereby maximizing the human’s latent reward function.

There has been only limited work tackling decision-maker heterogeneity [Nikolaidis et al., 2015, Hsiao et al., 2019, Li et al., 2017, Tamar et al., 2018]. For example, the approach by Nikolaidis et al. [2015] sought to divide demonstrators into relatively homogeneous clusters and learn a separate model of human decision-making from each cluster. As depicted in the center diagram in Fig. 1, this approach means that each model only has $1/k^{th}$ of the data from which to learn.

To overcome the data-inefficiency of such methods, Li et al. [2017] presented InfoGAIL, which used neural network-backpropagation to learn discrete, latent codes; however, InfoGAIL requires access to the environment model. Further, InfoGAIL only handles discrete modes rather than explicitly allowing for continuous variation. Hsiao et al. [2019] presented an approach to discover latent factors within demonstrations using a categorical latent variable. The discrete encoding used to represent the heterogeneity results in limited expressional power. Finally, Tamar et al. [2018] used a sampling-based approach to learn the modalities within the expert demonstrations, which requires a large set of data.

In this paper, we overcome these key gaps in prior work by providing an integrated learning framework that allows for learning planning policies from heterogeneous decision-makers. We propose using personalized embeddings, learned through backpropagation, which enables the apprenticeship learner to automatically adapt to a person’s unique characteristics while simultaneously leveraging any homogeneity that exists within the data (i.e., uniform adherence to hard constraints). We then present a human-interpretable version of our apprentice that allows for human interpretation of a given demonstrator’s behavior.

Finally, our approach leverages a neural network architecture based on the differentiable decision tree [Suárez and Lutsko, 1999]. Research combining neural networks and decision trees has been concerned with routing data appropriately so as to create subspaces more easily handled by sub-trees or

Algorithm 1 Personalized Neural Tree Training

Input: data $\vec{x}_p^t \in X$, labels $\hat{a}_p \in A$, embeddings $\omega \in \Omega$
Parameter: l -leaves, d -embedding length
Output: $f_{\theta|\omega}^{PNT*}, \omega_p$

- 1: Initialize $f_{\theta|\omega}^{PNT}, \Omega$
- 2: **for** i epochs **do**
- 3: $InputFeatures \leftarrow \text{Concatenate } \omega_p^{(i)} \text{ and } \vec{x}_p^t$
- 4: $a_p^t \leftarrow f_{\theta|\omega}^{PNT}(InputFeatures)$
- 5: $J_{\theta, \omega} = Loss_{Renyi}(a_p^t, \hat{a}_p^t)$
- 6: $\frac{\partial J_{\theta, \omega}}{\partial \theta}, \frac{\partial J_{\theta, \omega}}{\partial \omega} \leftarrow ComputeGradients(J_{\theta, \omega})$
- 7: $\omega_p^{(i+1)} \leftarrow \omega_p^{(i)} - \eta \frac{\partial J_{\theta, \omega}}{\partial \omega}$
- 8: $\theta^{(i+1)} \leftarrow \theta^{(i)} - \eta \frac{\partial J_{\theta, \omega}}{\partial \theta}$
- 9: **end for**
- 10: **return** $f_{\theta|\omega}^{PNT*}, \omega_p$

allow for faster inference [Laptev and Buhmann, 2014]. Researchers have also sought to combine classic decision trees with deep networks for faster training and intelligent initialization [Humbird et al., 2018].

3 Learning from Heterogeneous Decision

To learn from heterogeneous decision-makers, we must capture the homo- and heterogeneity among domain experts presenting varied demonstrations, allowing us to learn a general behavior model accompanied by personalized embeddings that fit distinct behavior modalities. Here, we present the framework for automatically synthesizing this model with personalized embeddings.

3.1 Personalized Neural Trees

Interpretability is an important area of exploration in machine learning, and an interpretable model of resource allocation or planning tasks would be useful for a variety of reasons, from decision explanations to training purposes. Therefore, we propose the use of differentiable tree-based architecture, which we term the Personalized Neural Tree (PNT) that can be converted to a decision tree in post-processing.

Our approach for training and testing is discussed in Algorithms 1 and 2. We begin with a balanced neural tree with 2^l leaf nodes and a demonstrator embedding. The demonstrator-specific embedding (represented by $\omega \in \Omega$) is concatenated with input data $\vec{x} \in X$ and routed directly to each decision node (as shown in Fig. 2), rather than being transformed between nodes as in a traditional deep network architecture. While this hinders the representation learning capacity of our model, it is important to learn a model directly over input features to preserve interpretability.

PNT Forward Pass – Each decision node in the PNT is conditioned on three differentiable parameters: a vector of weights $\vec{\beta} \in B$, a vector of comparison values $\vec{\phi} \in \Phi$, and a vector of selective importances $\vec{\psi} \in \Psi$. When input data \vec{x} is passed to a decision node y_i , the data is weighted by $\vec{\beta}_i$ and compared against $\vec{\phi}_i$ as shown in the inner multiplication in Equation 1. After comparison against $\vec{\phi}_i$, the model then

Algorithm 2 Personalized Neural Tree Testing

Input: data $\vec{x}_p^t \in X$, $f_{\theta|\omega}^{PNT^*}$, training embeddings mean $\bar{\Omega}$
Output: Demonstrator p 's action: a_p^t

- 1: $\omega_p^t = \bar{\Omega}$
- 2: **for** t in range(1, T) **do**
- 3: $InputFeatures = \text{Concatenate } \omega_p^t \text{ and } \vec{x}_p^t$
- 4: $a_p^t \leftarrow f_{\theta|\omega}^{PNT^*}(InputFeatures)$
- 5: $\hat{a}_p^t \leftarrow \text{ObserveDemonstratorAction}()$
- 6: $J_{\theta,\omega} = \text{Loss}_{\text{Renyi}}(a_p^t, \hat{a}_p^t)$
- 7: $\frac{\partial J_{\theta,\omega}}{\partial \omega} \leftarrow \text{ComputeGradients}(J_{\theta,\omega})$
- 8: $\omega_p^{(t+1)} \leftarrow \omega_p^{(t)} - \eta \frac{\partial J_{\theta,\omega}}{\partial \omega}$
- 9: **end for**

uses its selective importance vector $\vec{\psi}_i$ to decide which feature matters the most for y_i . The maximum value in $\vec{\psi}_i$ is set to 1, while all other elements of $\vec{\psi}_i$ are set to 0, and the inner parenthetical is transformed through a dot product with $\vec{\psi}_i$. This procedure ensures that each decision node only considers a single feature during each forward pass but still allows the model to learn over all features during backpropagation. Using vectors for weights, comparisons, and selectors means that every input feature in \vec{x} is considered individually, and the selector chooses just one to use for each forward pass, which helps convert the PNT into a decision tree later.

The single transformed feature is then weighted by a learned parameter α and passes through a sigmoid activation function. The sigmoid function ensures that each decision node y_i outputs a value between 1 and 0, where 1 means y_i evaluates to “true”, and 0 means that y_i evaluates to “false.” The learned parameter α enables the PNT to control the steepness of the sigmoid function, where an α of ∞ would represent a strict bound, as in a non-differentiable decision tree. To conclude, each decision node y_i evaluates Equation 1.

$$y_i = \sigma[\alpha(\vec{\psi}_i \cdot (\vec{\beta}_i \circ \vec{x} - \vec{\phi}_i))] \quad (1)$$

Leaf nodes L_i in the PNT maintain a set of weights over each output class and have exactly one path from root to leaf L_i . Decision nodes along the path output probabilities, which are all multiplied to produce the final probability of reaching L_i given input \vec{x} and the current demonstrator embedding ω_p . The set of weights in L_i is then multiplied by this probability, and the outputs of all leaves are summed to produce the final network output. An example is shown in Fig. 2 complete with an equation summarizing the output.

3.2 Training and Deployment

A Personalized Neural Tree (PNT) learns a model, $f_{\theta|\omega}^{PNT} : X \times \Omega \rightarrow [0, 1]^{|A|}$, of the human demonstrator's decision-making policy. $\theta \in \Theta(\Theta = \Psi \times B \times \Phi)$ is the policy weights and $\omega \in \Omega (\Omega \subset \mathbb{R}^d)$ is the demonstrator-specific personalized embedding of length d , which is a tunable hyperparameter. Since this personalized embedding is a continuous parameter, the outcome of choosing a length d that is too high or low in comparison to the optimum is not nearly as detrimental as choosing the non-optimal number of clusters in

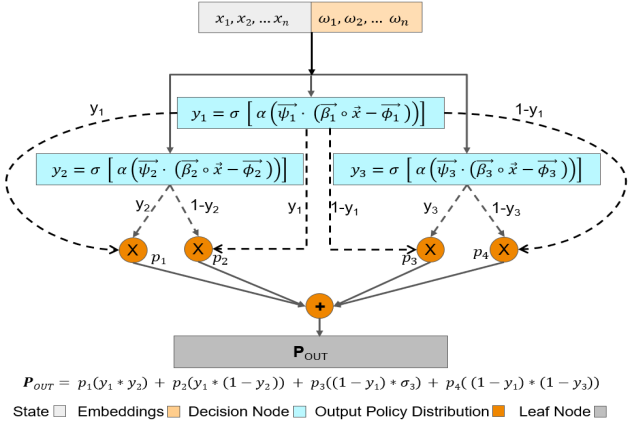


Figure 2: Personalized Neural Tree.

the approach of Nikolaidis et al. [2015] and Li et al. [2017]. The person-specific features ω identify the latent pattern of thinking for the current decision-maker.

The training procedure consists of taking as input an example of a state, x_p^t at time t , for person p as well as the person's embedding, $\omega_p^{(i)}$ at training iteration i , and predicting the person's action in that state, a_p^t , as shown in steps 2, 3, and 4 of Algorithm 1. The loss is computed as the Rényi divergence [Życzkowski, 2003] between the predicted action \hat{a}_p^t and the true action a_p^t . This loss is then backpropagated through the network to update model parameters θ and the personalized embedding ω via stochastic gradient descent, as shown in steps 5, 6, and 7. This process is repeated until a convergence criterion is achieved.

When applying the algorithm during runtime (i.e., testing) for a new human demonstrator p' , one updates the embedding $\omega_{p'}$; however, the model's parameters θ remain static. This utilizes the information provided after every timestep (i.e., the true action) to converge on the type of current demonstrator in embedding space. The personalized embedding $\omega_{p'}$ for a new human demonstrator is initialized to the mean demonstrator embedding of the demonstrators in the training set, as shown in step 1 of Algorithm 2. In other words, we start by assuming a new expert is performing the planning task as an average user; over time, we infer how she is acting differently and update our personalized embedding accordingly (through repetition of steps 3-8).

We note that researchers have explored the use of a latent embedding in other contexts [Killian et al., 2017, Tani et al., 2004]. Our approach is novel, however, in that we utilize a latent embedding as a personalized embedding for apprenticeship learning in domains with a high degree of freedom while also automatically inferring behavior, eliminating the need for tedious and biased annotation of person types. Furthermore, we present a natural method for online inference of a partner's preferences during runtime through updating ω_p .

3.3 Conversion to an Interpretable Tree

As machine learning is being increasingly deployed into the real world, interpretability is required for these systems to

gain human trust. Interpretability refers to attempts that help the user understand why a machine learning model behaves the way it does. A clear visualization of a robot’s policy is one way to help a human form an accurate representation of the robot’s capabilities [Paepcke and Takayama, 2010].

Most current work attempts to extract interpretability from deep networks through explanations of each layer [Olah et al., 2018] or by explanations generated through separate networks [Hendricks et al., 2018]. In our work, the Personalized Neural Tree is able to learn over datasets from heterogeneous demonstrators with high performance but still able to convert back into a simple, interpretable decision tree once learning has concluded, a process we term “discretization” (an example is shown in Fig. 3). This interpretable model is useful for understanding differences between demonstrators.

To achieve interpretability, we translate a PNT to a decision tree by using the selective importance parameters $\vec{\psi}$. Every decision node y_i in the PNT outputs a decision based on a single feature, chosen by $\vec{\psi}_i$; therefore, we can use $\vec{\psi}_i$ to choose which feature, weight, and comparison should be used to instantiate a new decision node for the interpretable decision tree. We can also remove the probabilistic weighting of leaves by pushing α towards infinity, restricting every decision’s output to 1 or 0. Finally, the class output within each leaf is chosen as the maximum value of the leaf’s weights. The new model is then a decision tree where every node considers one feature and outputs 1 or 0, only one leaf is selected for each forward pass, and each leaf outputs a single class.

Counterfactual Reasoning To increase the utility of our learning framework, we utilize counterfactual reasoning through pairwise comparisons, which has been commonly used in recommender systems [Page et al., 1998, Jin et al., 2008, Pahikkala et al., 2007] and increasingly leveraged in LfD [Gombolay et al., 2016, Brown et al., 2019]. Our approach utilizes Equations 2-3 to generate counterfactuals.

$$z_{a,a'}^{t,p} := [\omega_p, \bar{x}^t, \hat{x}_a^t - \hat{x}_{a'}^t], y_{a,a'}^t = 1 \quad (2)$$

$$z_{a',a}^{t,p} := [\omega_p, \bar{x}^t, \hat{x}_{a'}^t - \hat{x}_a^t], y_{a',a}^t = 0 \quad (3)$$

At each timestep, we observe the decision a that person p made at time t . From each observation, we then extract 1) the feature vector describing that action, x_a^t from state s^t , 2) the corresponding feature $x_{a'}^t$ for an alternative action $a' \in A | a' \neq a$, 3) a contextual feature vector capturing features common to all actions (e.g., how many workers are available to be assigned jobs) \bar{x}^t and 4) the person’s embedding ω_p . We note that each demonstrator has their own embedding which is updated through backpropagation.

Given this dataset, the apprentice is trained to output a pseudo-probability, $f(a, a', p)$ of action a being taken over action a' at time t by the human decision-maker p described by embedding ω_p , using features $z_{a,a'}^{t,p}$. To predict the probability of taking action a at timestep t , we marginalize over all other actions, as shown in Equation 4. Finally, the action prediction is the argument max this probability. We term models that use counterfactual reasoning as pairwise models.

$$\hat{P}(a|t, p) = \frac{\sum_{a' \in A} f(a, a', p)}{\sum_{a', a'' \in A} f(a', a'', p)} \quad (4)$$

4 Evaluation Environments

We use three environments to evaluate the utility of our personalized apprenticeship learning framework and display a discrete tree that can be used to explain the behavior contained within the learned models.

1) Synthetic Low-Dimensional Environment – The synthetic low-dimensional environment represents a simple domain where an expert will choose an action based on the state and one of two hidden heuristics. This domain captures the idea that we have homogeneity in conforming to constraints z and strategies or preferences (heterogeneity) in the form of λ . The idea is that decision-making exists on a manifold for each “mode” or “strategy” an operator shows, and we need to infer the identity of these manifolds through the embedding. This domain is a necessary building block to solving the “Synthetic Scheduling Environment” below. Demonstration trajectories are given in sets of 20 (which we denote a complete schedule), where each observation consists of $x^t \in \{0, 1\}$ and $z^t \in \mathcal{N}(0, 1)$, and the output is y^t . Exact specifications for the computation of the label are given by the observation of $y = x * \mathbb{1}_{(z>=0 \wedge \lambda=1) \vee (z<0 \wedge \lambda=2)}$, where $\mathbb{1}$ is the indicator function. Assuming a near-even class distribution, randomly guessing and overfitting to one class results in about 50% accuracy. Only by inferring the type of demonstrator, given by $\lambda_p \in \{1, 2\}$, will the learned policy be able to achieve an accurate model of decision-making.

2) Synthetic Scheduling Environment – The second environment we use is a synthetic environment that we can control, manipulate, and interpret to empirically validate the efficacy of our proposed method. For our investigation, we leverage a jobshop scheduling environment built on the XD[ST-SR-TA] scheduling domain defined by Korsah [2011], representing one of the hardest scheduling problems. In this environment, two agents must complete a set of 20 tasks which have upper- and lower-bound temporal constraints (i.e., deadline and wait constraints), proximity constraints (i.e., no two agents can be in the same place at the same time), and travel-time constraints. For the purposes of apprenticeship learning, an action is defined as the assignment of an agent to complete a task presently. The decision-maker must decide the optimal sequence of actions according to the decision-maker’s own criteria. For this environment, we construct a set of heterogeneous, mock decision-makers that schedule according to $\tau_i^* = \arg \max_{\tau_j \in \tau_S} (\rho_1 H_{EDF}(\tau_j) + \rho_2 H_{dist}(\tau_j) + H_{ID}(\tau_j, \rho_3))$.

In this equation, our decision-maker selects a task τ_i^* from the set of tasks τ_S . The task-prioritization scheme is based on three criteria: H_{EDF} prioritizes tasks according to deadline (i.e., “earliest-deadline first”), H_{dist} prioritizes the closest task, and H_{ID} prioritizes tasks according to a user-specified highest/lowest index or value based on ρ_3 (i.e., $\rho_3(j) + (1 - \rho_3)(-j)$). The heterogeneity in decision-making comes from the latent weighting vector $\vec{\rho}$. Specifically, $\rho_1 \in \mathbb{R}$ and $\rho_2 \in \mathbb{R}$ weight the importance of H_{EDF} and H_{dist} , respectively. Furthermore, $\rho_3 \in \{0, 1\}$ is a mode selector in which the highest/lowest task index is prioritized. By drawing $\vec{\rho}$ from a multivariate random distribution, we can create an infinite number of unique demonstrator types.

Environment	Our Method Interpretable Form ¹	Our Method	Sammut et al.	Nikolaidis et al.	Tamar et al.	Hsiao et. al.	InfoGAIL Li et. al.	Gombolay et. al.
Low-dim	89.15%	91.41%	56.54%	55.81%	54.50%	54.50%	57.87%	56.84%
Scheduling	100.00%	97.10%	5.00%	5.00%	8.65%	12.30%	31.19%	43.55%
Taxi	79.70%	89.02%	76.69%	76.69%	62.24%	76.78%	76.73%	76.69%

Table 1: A comparison of Heterogeneous LfD approaches. Our method achieves superior performance against all baseline approaches.

3) Taxi Domain – We utilize a variant of the Open AI Taxi Domain environment. Our environment has three locations: the village, the airport, and the city. The taxi driver has the objective of picking up a passenger from the city or village. There is always a passenger at the city, but the taxi driver may encounter up to 60 minutes of traffic going into the city. There may be a wait time of up to 60 minutes to pick up a passenger at the village; however, there is no traffic on the way to the village and the wait time is unknown to the taxi driver unless she is at the village. A dataset of 70 human-collected tree policies to solve this task (given with leaf node actions such as “Drive to the City”, “Drive to the Airport”, and “Wait for Passenger”, and decision node criterion depending on the amount of wait time, traffic time, and current location) are used to generate heterogeneous trajectories.

5 Results and Discussion

Several approaches are used in a thorough comparison between our personalized approach and those previous, including the approaches of [Sammut et al., 2002, Nikolaidis et al., 2015, Li et al., 2017, Tamar et al., 2018, Hsiao et al., 2019, Gombolay et al., 2016]. It should be noted that we utilize a simulation-free version of InfoGAIL, as the environment model is not available in many real-world domains. The accuracy metric during testing is multi-class classification accuracy. Note, during testing, the deployed model continuously updates its estimate of the demonstrator’s mode (utilizing the benchmark’s respective method for demonstrator mode inference, if it has one). We now evaluate our approach in the three domains to demonstrate that our approach sets a new state-of-the-art in heterogeneous LfD.

1) Synthetic Low-Dimensional Environment – A set of 50 schedules are given as input to the apprenticeship learning framework specified above. Row 1 of Table 1 shows that our method for learning a continuous, personalized embedding is the only state-of-the-art approach to solving even this simple classification problem. Our method was able to achieve 91.41% accuracy while the next-best method of Li et al. [2017] only achieves 57.87%, which is a 1.58-fold reduction in error. Even after discretizing to an interpretable form, our method is still able to achieve state-of-the-art performance. The inability of previous approaches to cope with

¹To infer the embeddings for the discrete, interpretable form of our PNT model, we utilize a pre-discretized version of the PNT to learn a given demonstrator’s embeddings, which is run prior or concurrently with the discretized version. The accuracy reported here is for the discretized model using the embeddings inferred by the pre-discretized PNT.

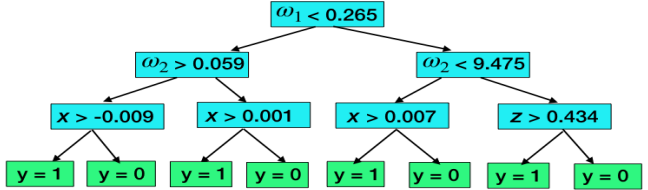


Figure 3: This figure depicts the learned PNT model after translation to an interpretable form for the low-dimensional environment, achieving 89.15% accuracy.

the dual-modality within this environment suggests that more data may be required for those approaches to work. InfoGAIL [Li et al., 2017] may also be suffering from mode collapse, a common issue in GAN-based frameworks. The interpretable PNT model, generated through the discretization methodology in Section 3.3, is shown in Fig. 3.

2) Synthetic Scheduling Environment – A set of 150 schedules generated by heterogeneous domain experts are given as input to the apprenticeship learning framework specified above. While we have the capability to generate a larger number of schedules, it is more significant to show that our framework works well on smaller training datasets, as in many cases these demonstrations can be expensive or sparse. The efficacy of each approach is shown in row 2 of Table 1, testing on 50 schedules from unseen demonstrators. Our personalized apprenticeship learning framework outperforms all other approaches, achieving near-perfect accuracy in predicting what task a domain expert will schedule. We achieve 97.10% accuracy while the next-best method of Gombolay et al. [2016] only achieves 43.55%, which is a 2.23-fold reduction in error. These results show that our Personalized Neural Trees can learn from observations in a high-dimensional and complex environment with heterogeneous demonstrators. After discretizing our method to an interpretable form, our method is able to achieve perfect accuracy, providing evidence that we can learn highly accurate models in a complex planning problem¹. Furthermore, the inability of other benchmarks that claim to handle heterogeneity [Li et al., 2017, Tamar et al., 2018, Hsiao et al., 2019] to learn proficient behavior suggests that they either may require more data, are unable to handle the complexity associated with planning problems simultaneously with heterogeneity, or require highly distinct demonstrator modalities.

3) Taxi – Across our 70 users, we train models using 25 trajectories from each user, and test on a holdout set of 25 successful trajectories. As seen in row 3 of Table 1, our personalized apprenticeship learning framework outperforms all other

benchmarks and is the only method to achieve over 80%. This reaffirms that our framework can outperform state-of-the-art benchmarks in a real-world planning problem. Even after discretizing to an interpretable form, our method is still able to achieve state-of-the-art performance. We speculate that all other methods overfit to the most prevalent behavior represented among the 70 users, and are unable to take advantage of the heterogeneity represented within the training dataset.

6 Interpretability User Study

Thus far, we have shown across a variety of datasets that our counterfactual PNT algorithm is able to achieve state-of-the-art performance in learning from heterogeneous decision-makers. Further, we have shown that our PNT algorithm can be directly converted into a discrete decision tree. Our primary goal has been to achieve both high performance and interpretability. To achieve this latter goal, we assess whether this counterfactual model is useful in the hands of end users. Accordingly, we conducted a novel user study to assess the interpretability of our framework against a neural network using the same approach. As our goal is to present our learned behavior model in an interpretable fashion, we assess which type of decision-making framework is most interpretable.

The neural network models and decision trees in our study are generated by performing LfD to learn heterogeneous behavior policies in a very simple scheduling domain. In this domain, synthetics schedulers are given utilities of three tasks and must choose the highest or lowest task index based on a pre-specified latent decision-making criteria. Tree models are generated using our PNT framework and discretized to produce decision trees. The neural network models are generated by appending our personalized embeddings to a neural network and following the same training and testing methodology described in Algorithms 1 and 2. All models were trained until they achieved similar testing accuracy while minimizing model size. Then, comparison weights and model weights for the discrete trees and neural networks, respectively, were rounded to the nearest 0.5. Rounding yielded $\sim 5\%$ loss in accuracy but allowed for the survey to be conducted within a reasonable time. We explore the hypotheses stated below.

Hypothesis 1 (H1): *Tree-based decision-making models are more interpretable than neural-network based models.* To test this hypothesis, we ask users to answer a Likert scale questionnaire after utilizing each decision-making framework to make predictions from a set of inputs.

Hypothesis 2 (H2): *Tree-based decision-making models are quicker to validate than neural-network based models.* To test this hypothesis, we record the time required for a user to compute the model's output given a set of inputs.

Hypothesis 3 (H3): *Tree-based decision-making models are more easily utilized than neural-network based models.* To test this hypothesis, we measure the user's ability to correctly determine the model's output given a set of inputs.

6.1 Methods and Materials

We designed an online questionnaire which asks users to make predictions following each a decision tree and a neural network. For each type of decision-making framework,

we provide instructions for how to utilize the framework to make a prediction. The order in which the user completes the neural network portion and decision tree portion is randomized. In both cases, users have to trace several inputs to compute an output which leads them to choose a task to schedule. In addition, we ask subjects to respond to Likert scale questionnaires to gauge their subjective perception of both the model interpretability and overall process interpretability, and record completion times.

6.2 User Study Results and Discussion

Analysis of H1 – We test for normality and homoscedasticity and do not reject the null hypothesis in either case, using Shapiro-Wilk ($p > 0.2$ and $p > 0.05$, respectively) and Levene's Test ($p > 0.6$ and $p > 0.9$, respectively). We perform a paired t-test and find that tree-based models were rated statistically significantly higher than neural networks on users' Likert scale ratings for model interpretability and overall process interpretability ($p < 0.03$ and $p < 0.04$, respectively).

Analysis of H2 – We perform a Wilcoxon signed-rank test on the per-model time to determine an output given a set of inputs and find that tree-based models were statistically significantly quicker to validate than neural networks ($p < 0.001$).

Analysis of H3 – We test for normality and homoscedasticity and do not reject the null hypothesis in either case, using Shapiro-Wilk ($p > 0.1$) and Levene's Test ($p > 0.05$). We perform a paired t-test and find that users using tree-based models statistically significantly achieved higher overall correctness scores compared to neural network based models ($p < 0.05$), supporting **H3**.

Take-away – These data support all of our hypotheses (**H1**, **H2**, and **H3**). Positively, our PNT method is more interpretable, easier to follow, and quicker to validate than neural network models. Given these positive results, we believe our model provides a new state-of-the-art in accuracy for heterogeneous LfD (Table 1) and also a strong step towards making such models more interpretable.

7 Conclusion

We present an apprenticeship learning framework for learning from heterogeneous demonstrators, leveraging a Personalized Neural Tree that is able to capture the homo- and heterogeneity among human domain experts presenting varied trajectories through the use of personalized embeddings. The design of our PNT allows for translation into an interpretable form while maintaining a high level of accuracy. These discrete trees can be used to provide valuable insights into a demonstrator's decision-making behavior. Furthermore, we demonstrate that our approach is notably superior to standard apprenticeship learning models and several approaches used in multi-modal behavior learning in synthetic and real-world domains. We conduct a user study to assess the interpretability of our discretized trees and neural networks and find that our discrete trees are more interpretable, easier to follow, and quicker to validate than neural networks.

References

Umang Bhatt, Alice Xiang, Shubham Sharma, Adrian Weller, Ankur Taly, Yunhan Jia, Joydeep Ghosh, Ruchir Puri, José M. F. Moura, and Peter Eckersley. Explainable machine learning in deployment, 2019.

Daniel S. Brown, Wonjoon Goo, Prabhat Nagarajan, and Scott Niekum. Extrapolating beyond suboptimal demonstrations via inverse reinforcement learning from observations. In *ICML*, 2019.

Matthew Gombolay, Reed Jensen, Jessica Stigile, Sung-Hyun Son, and Julie Shah. Decision-making authority, team efficiency and human worker satisfaction in mixed human-robot teams. In *Proceedings of the International Joint Conference on Artificial Intelligence (IJCAI)*, New York City, NY, U.S.A., July 9-15 2016.

Lisa Anne Hendricks, Ronghang Hu, Trevor Darrell, and Zeynep Akata. Generating counterfactual explanations with natural language. *arXiv preprint arXiv:1806.09809*, 2018.

Fang-I Hsiao, Jui-Hsuan Kuo, and Min Sun. Learning a multi-modal policy via imitating demonstrations with mixed behaviors. *ArXiv*, abs/1903.10304, 2019.

Kelli D Humbird, J Luc Peterson, and Ryan G McClaren. Deep neural network initialization with decision trees. *IEEE transactions on neural networks and learning systems*, 2018.

Rong Jin, Hamed Valizadegan, and Hang Li. Ranking refinement and its application to information retrieval. In *Proceedings of the 17th International Conference on World Wide Web, WWW '08*, pages 397–406, New York, NY, USA, 2008. ACM. ISBN 978-1-60558-085-2.

Taylor W Killian, Samuel Daulton, George Konidaris, and Finale Doshi-Velez. Robust and efficient transfer learning with hidden parameter markov decision processes. In I. Guyon, U. V. Luxburg, S. Bengio, H. Wallach, R. Fergus, S. Vishwanathan, and R. Garnett, editors, *Advances in Neural Information Processing Systems 30*, pages 6250–6261. Curran Associates, Inc., 2017.

G. Ayorkor Korsah. *Exploring bounded optimal coordination for heterogeneous teams with cross-schedule dependencies*. PhD thesis, Carnegie Mellon University, Pittsburgh, PA, January 2011.

Dmitry Laptev and Joachim M Buhmann. Convolutional decision trees for feature learning and segmentation. In *German Conference on Pattern Recognition*, pages 95–106. Springer, 2014.

Benjamin Letham, Cynthia Rudin, Tyler H McCormick, David Madigan, et al. Interpretable classifiers using rules and bayesian analysis: Building a better stroke prediction model. *The Annals of Applied Statistics*, 9(3):1350–1371, 2015.

Yunzhu Li, Jiaming Song, and Stefano Ermon. Infogail: Interpretable imitation learning from visual demonstrations. In I. Guyon, U. V. Luxburg, S. Bengio, H. Wallach, R. Fergus, S. Vishwanathan, and R. Garnett, editors, *Advances in Neural Information Processing Systems 30*, pages 3812–3822. Curran Associates, Inc., 2017.

Stefanos Nikolaidis, Ramya Ramakrishnan, Keren Gu, and Julie Shah. Efficient model learning from joint-action demonstrations for human-robot collaborative tasks. In *Proceedings of the Tenth Annual ACM/IEEE International Conference on Human-Robot Interaction, HRI '15*, pages 189–196, New York, NY, USA, 2015. ACM.

Chris Olah, Arvind Satyanarayanan, Ian Johnson, Shan Carter, Ludwig Schubert, Katherine Ye, and Alexander Mordvintsev. The building blocks of interpretability. *Distill*, 3(3):e10, 2018.

Steffi Paepcke and Leila Takayama. Judging a bot by its cover: An experiment on expectation setting for personal robots. In *Proceedings of the 5th ACM/IEEE International Conference on Human-robot Interaction, HRI '10*, pages 45–52, Piscataway, NJ, USA, 2010. IEEE Press. ISBN 978-1-4244-4893-7.

L. Page, S. Brin, R. Motwani, and T. Winograd. The pagerank citation ranking: Bringing order to the web. In *Proceedings of the 7th International World Wide Web Conference*, pages 161–172, Brisbane, Australia, 1998. URL citeseer.nj.nec.com/page98pagerank.html.

Tapio Pahikkala, Evgeni Tsivtsivadze, Antti Airola, Jorma Boberg, and Tapio Salakoski. Learning to rank with pairwise regularized least-squares. *SIGIR 2007 Workshop on Learning to Rank for Information Retrieval*, 01 2007.

Claude Sammut, Scott Hurst, Dana Kedzier, and Donald Michie. *Learning to Fly*, page 171–189. MIT Press, Cambridge, MA, USA, 2002.

Alberto Suárez and James F Lutsko. Globally optimal fuzzy decision trees for classification and regression. *IEEE Transactions on Pattern Analysis and Machine Intelligence*, 21(12):1297–1311, 1999.

Aviv Tamar, Khashayar Rohanimanesh, Yinlam Chow, Chris Vigorito, Ben Goodrich, Michael Kahane, and Derik Pridmore. Imitation learning from visual data with multiple intentions. In *International Conference on Learning Representations*, 2018.

Jun Tani, Masato Ito, and Yuuya Sugita. Self-organization of distributedly represented multiple behavior schemata in a mirror system: Reviews of robot experiments using rmnpb. *Neural networks : the official journal of the International Neural Network Society*, 17:1273–89, 10 2004.

Karol Życzkowski. Rényi extrapolation of shannon entropy. *Open Systems & Information Dynamics*, 10(03):297–310, 2003.